advances in Technology

Adv. Technol. 2025, 5(2), 119-131

Full Paper

Optimizing Electrode Geometry for Enhanced Cell Separation Using Dielectrophoresis: A Study on Fillet Radius Impact

Thisakya Ransarani*, Dumith Jayathilaka, and Ranjith Amarasinghe

Department of Mechanical Engineering, University of Moratuwa, Katubadda 10400, Sri Lanka

Corresponding Author: thisakya2k@gmail.com

Received: 26 November 2024; Revised: 11 February 2025; Accepted: 11 February 2025; Published: 20 June 2025

Abstract

This paper presents a dielectrophoresis-based device designed for separating platelets from red blood cells (RBCs), utilizing the size difference between the cells to induce negative dielectrophoretic behavior to achieve effective separation. The study employs Alternating Current Dielectrophoresis (AC-DEP) at a frequency of 100 kHz, modelling the cells with defined parameters using COMSOL Multiphysics 5.3a simulations. The objective is to investigate the effect of varying electrode geometry, specifically the curvature at the corners of the electrodes, on cell separation performance. By adjusting the curvature of the sidewall electrodes through varying the fillet radius between 0μm and 18μm, the study observes how these changes influence the electric field and, consequently, the separation of RBCs and platelets. Results demonstrate that altering electrode geometry improves separation performance by optimizing electric field distribution and cell trajectories.

Keywords: cell separation, comsol, dielectrophoresis, electrode geometry

Introduction

Cell separation plays a vital role in biomedical research and clinical diagnostics, providing the ability to isolate specific cell types from heterogeneous populations of cells [1]. This ability to precisely separate cell types is necessary for numerous applications such as disease diagnostics, therapeutic procedures and the study of cell behavior [2]. In particular, isolating cell types such as platelets and red blood cells (RBCs) are essential. Platelets serve a wide range of functions in human physiology. They play a crucial role in preventing excessive blood loss at locations of vascular injury and release substances that support tissue repair and immune responses. Clinically, platelets are essential for accelerating the healing process [3]. Platelet transfusions are often used for this acceleration process and to prevent death due to significant blood loss in patients with low platelet counts. In the context of cancer treatment, platelet transfusions enable more aggressive chemotherapy regimens, potentially improving treatment effectiveness [4]. Given the role of platelets, accurate measurement of platelet concentration and, when necessary, isolation of platelets from blood are essential. Meanwhile, RBCs are the predominant cell type in human blood. They transport oxygen from the lungs to the body and carbon dioxide from the body to the lungs for exhalation. Several conditions are linked to defects in RBCs, such as abnormalities in their size, shape, or viscoelastic

properties. Common disorders associated with RBCs include anemias such as sickle cell anemia and hemolytic anemia [5, 6]. To diagnose and study these abnormalities, healthcare professionals employ complete blood count and cell isolation techniques.

Cell separation can be achieved using a variety of techniques, ranging from traditional macro-scale methods to more recent innovations. Among these, MEMS (Micro-Electro-Mechanical Systems) has gained significant attention over macro-scale systems due to its advantages in handling smaller sample volumes, reduced cost, enhanced portability, and the ability to be integrated with other analytical techniques, offering more precise and efficient separation capabilities [7]. Point-of-care (POC) devices are diagnostic tools designed for quick and simple testing at the site of patient care. MEMS play a crucial role in the advancement of POC devices, enabling miniaturization and improved diagnostic capabilities [1, 8]. Since the 1950s, MEMS technology has undergone significant development, evolving to facilitate precise cell separation through various methods, including optical, magnetic, electrical, and acoustic techniques [9, 10]. Dielectrophoresis (DEP) is a widely used electrical method for cell separation due to its ability to separate neutral cells without labeling and in a non-destructive manner. DEP-based devices are capable of achieving high recovery and purity standards in cell separation [11, 12]. Numerous studies have been conducted on cell separation using DEP. Sharp-ended electrodes are a common configuration in DEP devices. N. Lewpiriyawong and C. Yang (2012) developed a model featuring sidewall composite rectangular electrodes for the continuous separation of submicron and micron particles using AC-DEP [13]. Nguyen *et al.,* (2021) presented a study featuring a model with an improved channel structure to determine the optimal parameters for separating circulating tumor cells from RBCs using an array of coplanar microelectrodes. Çetin et al., (2009) designed a device for the continuous separation of yeast cells, white blood cells, and latex particles of varying sizes [14]. Their design uses two asymmetric, three-dimensional electrodes: one triangular and the other rectangular, achieving 100% separation efficiency. Several studies have also explored the impact of electrode geometry on cell separation. Y. Zhang and X. Zhang and Chen (2020) analyzed the effects of varying electrode shapes, applied voltages, and exit angles on the separation of platelets from RBCs [15]. Varmazyari *et al.,* (2022) conducted experiments using three distinct sidewall electrode configurations to evaluate the separation performance of MDA-MB-231 cancer cells from different white blood cell subtypes [16].

Although current methods demonstrate effectiveness, they are constrained by several limitations. Joule heating [17], low throughput [14], particle adhesion [18], and microchannel clogging [19] are among the key challenges associated with DEP. These challenges arise from various factors, such as the application of high voltages, reduced separation efficiency at high flow rates, and particle accumulation within the system. Addressing these limitations is important for enhancing the performance of DEP-based cell separation technologies.

The study in this paper aims to address these gaps by enhancing the cell separation performance by altering the electrode geometry a previous study. The previous study successfully separates platelets in continuous flow by employing a combination of hydrodynamic and DEP forces, utilizing a voltage of 10V and a frequency of 100 kHz. The fabricated device demonstrates highly efficient separation, achieving a platelet

purity of 98.8% with less than 2% cell loss [20]. Our study simulates the impact of altering the electrode structure, specifically by altering the curvature to create a more concave electrode. Due to DEP sensitivity to particle size, it is an ideal technique for the separation of RBCs and platelets [14]. By enhancing the design, this study has the potential to advance DEP-based devices, making them more reliable and capable of delivering faster results.

The following sections of this manuscript provide an overview of the fundamental principles used for the study and its relevance for cell separation. This is followed by a detailed discussion of the proposed design, focusing on electrode geometry modifications and the associated simulation methodology. Results from COMSOL Multiphysics 5.3a simulations are then presented and analyzed, demonstrating the impact of electrode curvature on separation performance. Finally, the broader implications of these findings for DEP-based technologies are discussed, along with potential areas for improvement and future research directions.

Theory

DEP is the phenomenon of the movement of polarizable particles when exposed to a non-uniform electric field. For a neutral particle exposed to a uniform electric field, the electrostatic forces acting on the opposite ends of the dipole are equal, resulting in no net force for movement. However, when the electric field is non-uniform, the forces on the ends of the dipole differ, creating a net force that causes the particle to move [12, 21, 22]. The time-averaged DEP force acting on a spherical particle with a radius r, suspended in a medium with a permittivity of ε_m, exposed to an electric field with root mean square value E_{rms}, is calculated using Equation (1).

$$F_{DEP} = 2\pi\varepsilon_m r^3 \mathrm{Re}[f_{CM}]\nabla|E_{rms}|^2 \quad \text{Equation (1)}$$

$\mathrm{Re}[f_{CM}]$, refers to the real part of the Clausius-Mossotti factor, f_{CM}. The factor is a frequency-dependent function [23] given by Equation (2).

$$f_{CM} = \frac{\varepsilon_p^* - \varepsilon_m^*}{\varepsilon_p^* + 2\varepsilon_m^*} \quad \text{Equation (2)}$$

Where the ε_p^* and ε_m^*refers to the complex permittivity of the cells and medium, respectively. The complex permittivity can be calculated by Equation (3).

$$\varepsilon^* = \varepsilon - \frac{j\sigma}{\omega} \quad \text{Equation (3)}$$

Where σ represents the electrical conductivity, j is the imaginary unit, and ω denotes the electric field's angular frequency [12, 21, 22]. If the electrical polarizability of the cells exceeds the polarizability of the suspending medium, the DEP force will act in the same direction as the gradient of the electric field, resulting in positive dielectrophoresis (PDEP). Alternatively, if the suspending medium's polarizability is higher, the DEP force drives the cells in the opposite direction, toward the weaker electric field regions, leading to negative dielectrophoresis (NDEP) [21, 23]. NDEP and PDEP can also be defined based on the $\mathrm{Re}[f_{CM}]$ value, which varies between -0.5 and 1 [15]. If it is negative cells experience NDEP and if positive

cells experience PDEP [24]. In addition to the DEP force, the viscous force is considered in the design. Other forces, such as inertial and gravitational forces, can be assumed to be negligible [15]. The opposing Stokes drag force experienced by a spherical particle with radius r, moving at a velocity v in a fluid with viscosity η, can be calculated using Equation (4) [17].

$$F_{Drag} = 6\pi\eta rv \qquad \text{Equation (4)}$$

DEP can be influenced using both DC and AC electric fields. When the electric field is DC the field doesn't oscillate and it has a constant direction. In contrast, AC electric fields oscillate, providing a dynamic force to the particles. In DC-DEP, the force primarily depends on the properties of the particle and the medium, as well as the gradient of the electric field [17]. In AC-DEP, in addition to these parameters, the frequency of the applied electric field also contributes to determining the force experienced by the particles [12]. This frequency dependence enables selective manipulation of particles using AC-DEP. This study uses AC-DEP, where both cell types experience NDEP. Given that the volume of RBCs is approximately ten times larger than that of platelets, and considering that the DEP force is proportional to the particle radius, RBCs experience a significantly stronger NDEP force. Consequently, RBCs are deviated more from high electric fields, while platelets, experiencing a comparatively weaker NDEP force, experience less deviation. This difference effectively separates RBCs from platelets based on their size-dependent DEP behavior.

Design and Simulation

Building upon the design outlined in [20], the model was developed from the ground up for this study, incorporating necessary modifications and optimizations.

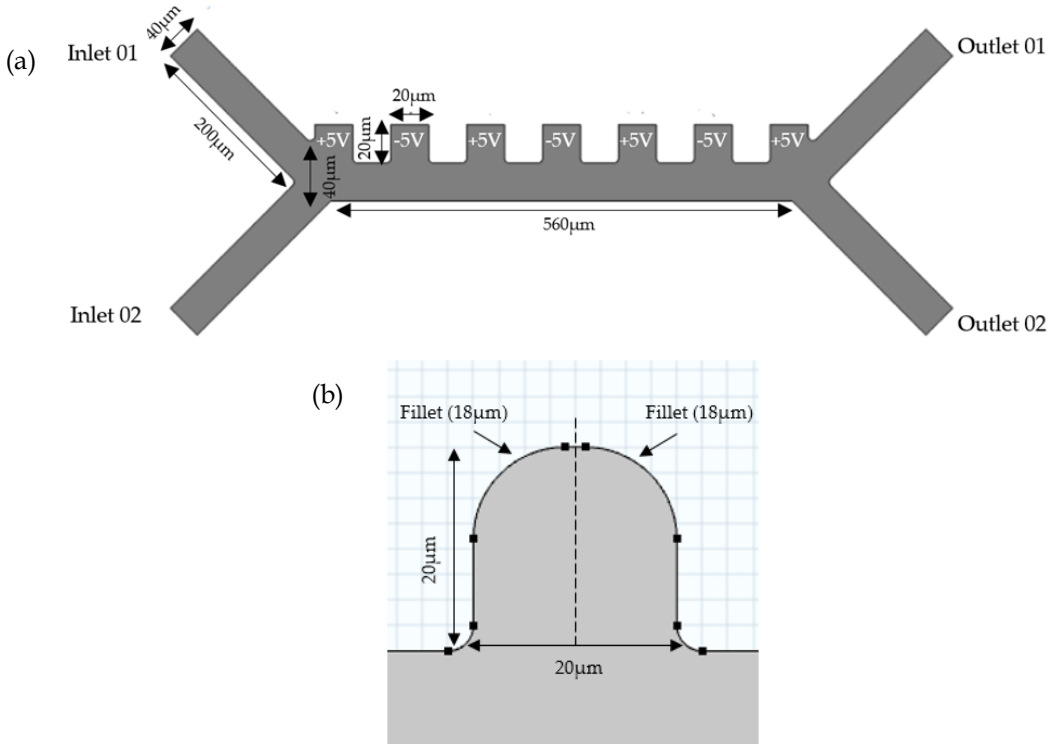

Figure 1. (a) 2D model for the micro device and (b) electrode design with rounded corners (fillets)

This approach facilitated a comprehensive understanding of the original design and its underlying principles. The system consists of three regions: injection region with two inlets, a separation region and a collection region with two outlets. The microchannel is designed in a configuration similar to a combined H-filter arrangement where the electric field is generated by electrodes with alternating polarities, applying a voltage magnitude of 5V. The electrodes in the study initially have sharp ends with dimensions of 20μm by 20μm. Considering the extension of the same electrode design along the other axis, the device can be effectively modelled as a 2D model, shown in Figure 1(a). This simplification assumes uniformity along the extended axis. The separation region has a length of 560μm and a height of 40 μm. The inlets and outlets have dimensions of 40 μm width and 200 μm height.

Inlet 1 introduces a mixture containing RBCs and platelets, while inlet 2 introduces the buffer solution, with flow velocities of 134 μm/s and 853 μm/s [15], respectively. The buffer solution acts as a medium that impacts how the electric fields interact with the cells, influencing the DEP forces applied to them. Additionally, it functions as the carrier fluid, facilitating the transport of RBCs and platelets through the microfluidic channels. The as the study's frequency is 100 kHz, where both types of cells experience NDEP force. Due to the differing forces experienced by the two particle types, platelets will be directed towards outlet 01, and RBCs will be directed towards outlet 02. The number of RBCs and platelets in the simulation is defined as 400 and 160, respectively, factors such as the natural abundance of these cell types in blood, optimization of computation time, and the need for a sufficient sample size to assess exit times accurately were considered.

COMSOL Multiphysics 5.3a is used for the simulation purposes, it allows the integration of numerous physics to model real-world phenomena. Numerous studies have employed this software for DEP-based applications such as the continuous separation of polystyrene beads and Hela cells using AC-DEP [25], as well as the trapping and concentration of yeast cells from a large sample volume into a smaller volume using carbon-electrode DEP [26]. The model development incorporates three physics modules: Creeping Flow to simulate the fluid flow, Electric Currents for the generation of the electric field, and the Particle Tracing for Fluid Flow is used to model the particle trajectories under the effect of forces. DEP and Drag forces were defined using the forces within the Particle Tracing for Fluid Flow physics interface in COMSOL. The drag force was modeled using Stokes' law. Electric insulation is applied to all boundaries of the device except at the electrode boundaries. The voltage applied is +5 V and -5 V alternately across an array of 7 electrodes, starting with a positive electrode. To simulate particle interactions with the device walls, a bounce condition was applied to all boundaries except for the outlets. When particles contact the outlet walls, they were assumed to freeze. For the fluid flow, a no-slip condition was applied to the device walls, excluding the inlet and outlet boundaries. The particles were modeled as solid, non-charged entities having the properties [15] displayed in Table 1. The suspending fluid in which the particles are immersed has a conductivity of 55mS/m and a relative permittivity of 80 [15]. The simulation consisted of three studies. Study 1 included two steps: a stationary study step to solve for the fluid flow, followed by a frequency-domain study step to solve for the electric potential within the microchannel. Study 2 involved a time-dependent analysis without the presence of DEP forces, while Study 3 was conducted under the

influence of DEP forces. Both Studies 2 and 3 were solved for the particle tracing fluid flow to evaluate particle dynamics.

Table 1. Properties of Platelets and RBCs

Cell type	Conductivity [S/m]	Relative Permittivity	Diameter [μm]	Shell conductivity [S/m]	Shell Relative Permittivity	Shell Thickness [nm]
Platelets	0.25	50	1.8	1E-6	6	8
RBCs	0.31	59	5	1E-6	4.44	9

As stated, numerous studies have explored the influence of electrode shape modification on particle separation [15, 16]. These investigations have demonstrated the beneficial impact of optimized electrode geometry in enhancing separation performance. This study plans to modify the sharp edges of the electrodes by curving them to investigate the impact on separation performance. Figure 1(b) illustrates the 2D schematic of the electrode with rounded corners, resulting from the introduction of fillets. The addition of the fillets at the corners has modified the original square shape of the electrode. The fillet radius of the electrodes is varied from 0 to 18μm in 3μm intervals to evaluate how these changes influence the cell separation performance. Given the electrode dimensions of 20 μm × 20 μm, the maximum allowable fillet size is 18 μm. Fillet sizes were varied in 3 μm intervals to systematically study their impact on performance. Figure 2 presents the simulation model incorporating an 18 μm fillet radius.

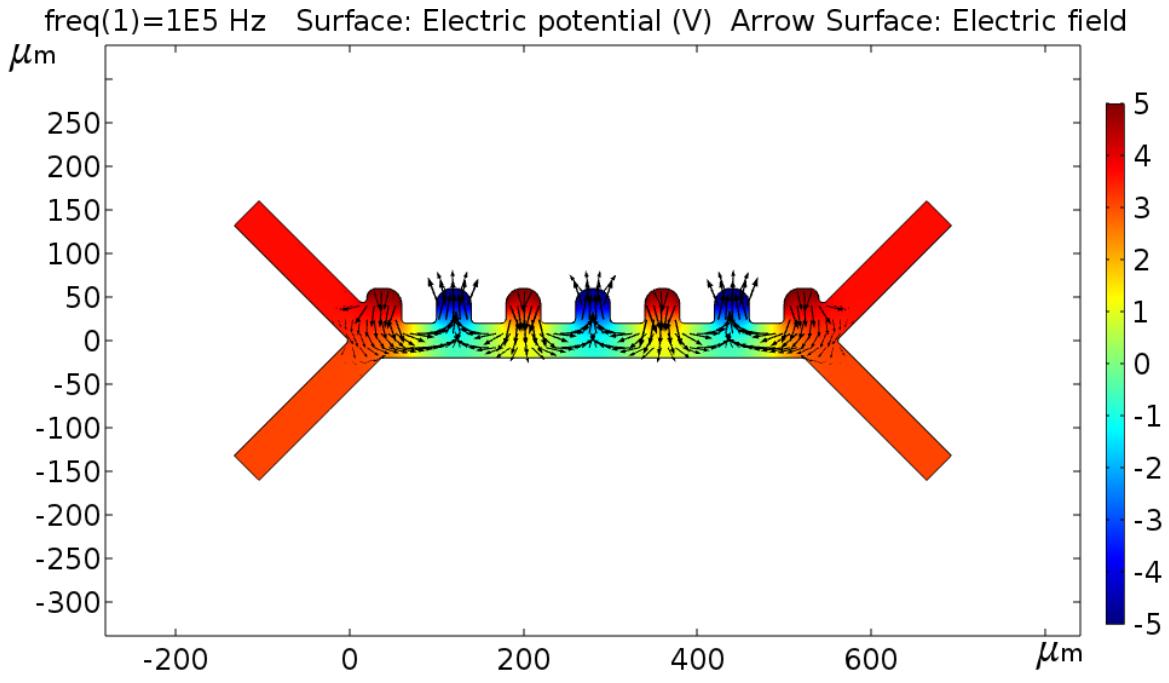

Figure 2. Electrode geometry model with an 18 μm fillet radius

Additionally, Figure S1 to S6, provided in the support information section, includes the simulation models for each electrode, corresponding to incremental changes in fillet radius at 3 μm intervals. The arrows indicate the direction of the electric field, illustrating how it varies across the separation region. All the parameters are kept constant throughout the study, except for the fillet radius of the electrodes. By isolating the fillet radius as the variable factor, the study aims to precisely assess how electrode geometry changes influence the electric field's behavior and, consequently, the particle separation performance. The recorded time intervals of the simulation have a resolution of 2 ms.

Two accumulators were implemented at the two outlet boundaries. The accumulator type was set to 'count,' and the accumulate over was defined as 'particle-wall interactions.' The accumulators summed the particles that reached the respective boundaries. A global evaluation was then performed to compute the total accumulated particle count. The accumulated number of particles at each time step was recorded at 2 ms intervals. The earliest time at which the particle count stabilized to a constant value was identified as the separation time. The separation efficiency of the process was calculated by comparing the number of particles of each type collected at the outlets with the initial number of particles injected into the system.

A similar study conducted with a comparable model concluded that while the grid number did not significantly affect the electric field distribution, it had a measurable influence on fluid velocity. That study selected a mesh with 7,894 elements [15]. In this study, where the primary focus is on the electric field, a mesh of 7,776 elements was selected to balance simulation accuracy and computational efficiency. The chosen mesh is a physics-controlled mesh with a normal element size, including 7,159 triangular and 617 quadrilateral elements. The average skewness quality measure for this configuration is 0.8079, with an average growth rate of 0.7328. Additionally, physics-controlled meshes with fine and coarse element sizes were tested for comparison. The fine mesh improved the quality to 0.8165 with 9,386 elements, while the coarse mesh reduced the quality to 0.7928 with 4,728 elements. Ultimately, the mesh with 7,776 elements and a quality measure of 0.8079 was selected as an optimal compromise, ensuring reliable simulation results while minimizing computational demands.

Results and Discussion

When the system is modeled without the influence of the DEP force, RBCs and platelets follow the same trajectory, exiting through outlet 01, as illustrated in Figure 3(a). When the DEP force is introduced the platelets exited through outlet 01, while the RBCs exited through outlet two as demonstrated in Figure 3(b).

The increase in the fillet size led to a reduction in the separation time. The average reduction in separation time was calculated as 1.89 ms/μm for platelets and 1.78 ms/μm for RBCs. A direct correlation between the fillet size and the separation time was observed, as illustrated in Figure 4.

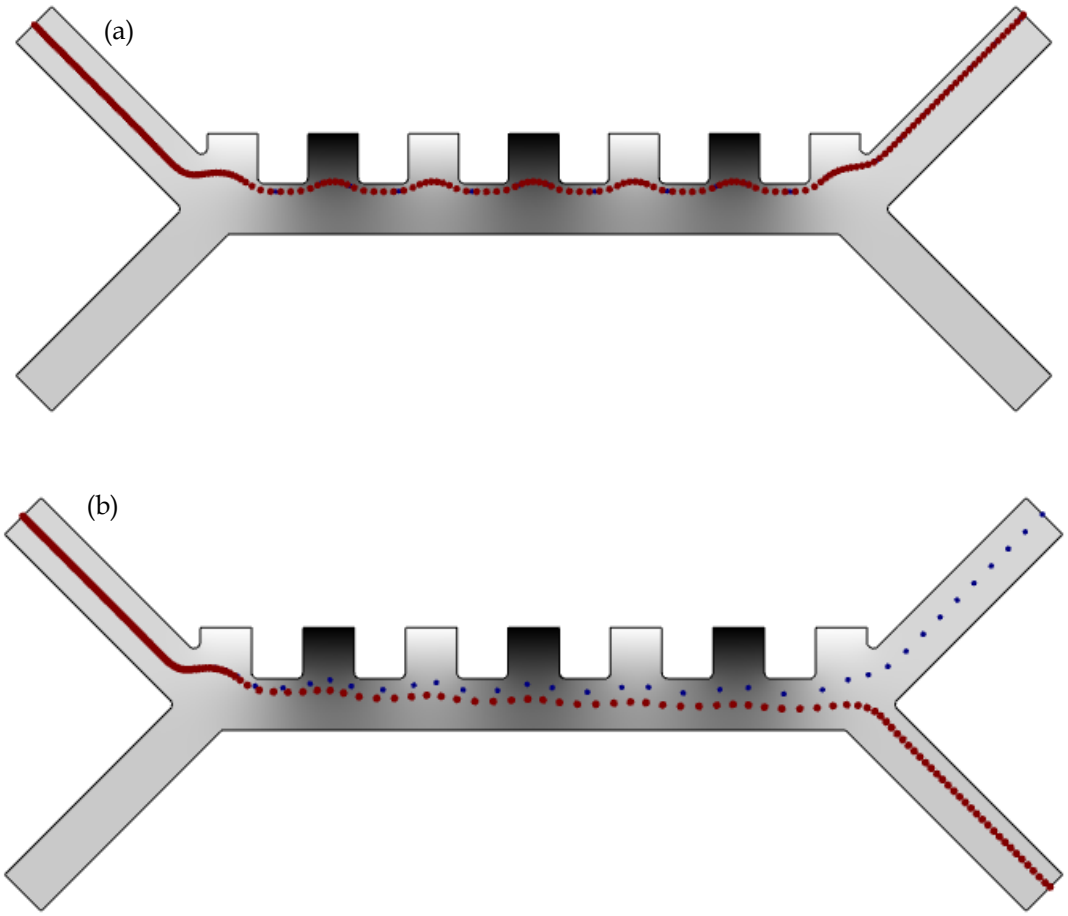

Figure 3. (a) Simulated particle trajectories in the absence of DEP forces and (b) Simulated particle trajectories under the influence of DEP forces

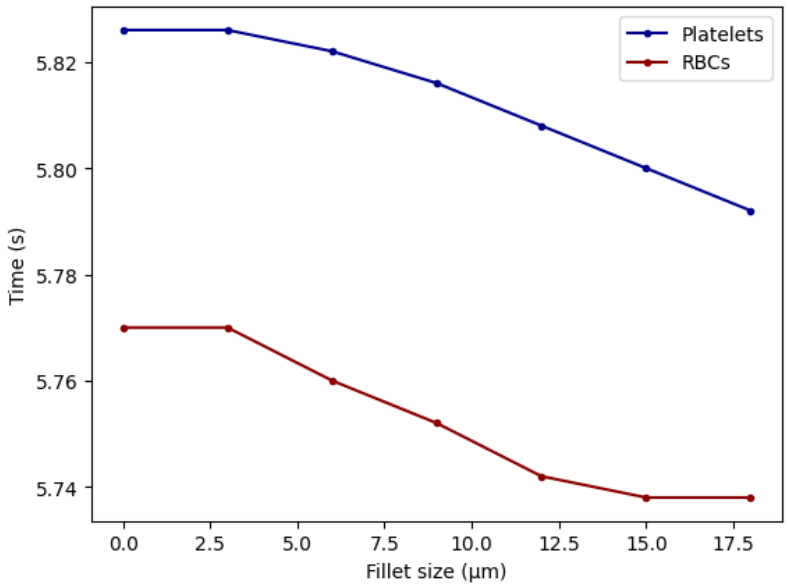

Figure 4. Separation time vs fillet radius graph

To comprehend the underlying cause of the observed, Equation (1) was analyzed. Given that all other parameters are constant, the only variable influencing the force can be considered to be the root mean square value of the electric field. Therefore, the voltage distribution along a specified axis was examined for all fillet sizes, as illustrated below. The separation efficiency (SE) was calculated using Equation (5) for the simulation. For all fillet sizes tested, the separation efficiency was 100%. This indicates that all particles of the same type were successfully collected at their designated outlet.

$$\text{SE} = \frac{\text{Number of particles at the outlet}}{\text{Number of particles injected}} \qquad \text{Equation (5)}$$

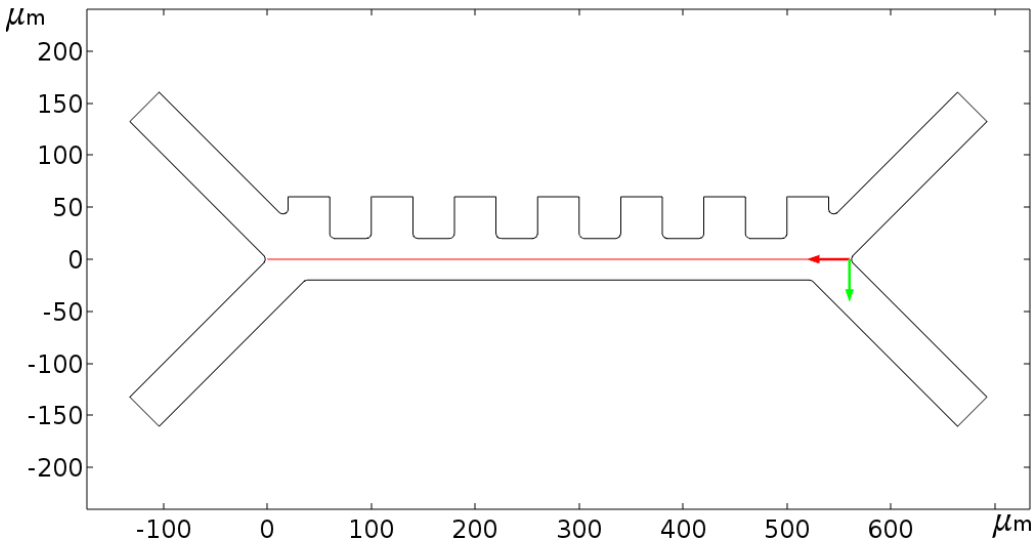

Figure 5. 2D cutline along the microchannel

As depicted in Figure 5, a 2D cutline was established along the centerline of the separation region, extending along its length (0 - 560 μm). This cutline serves as a reference for analyzing and comparing the voltage potential variations across different fillet configurations within the separation channel. Table 2 presents the maximum and minimum voltages corresponding to each fillet size, demonstrating an enhancement in voltage magnitude as the fillet size increases.

Figure 6 shows the electric potential variation along the separation channel for each fillet type based on the 2D cutline. The y-axis of the graph represents the electric potential, while the x-axis indicates the arc length corresponding to the microchannel length. These graphs provide a detailed view of how the electric potential varies with electrode geometries, highlighting that the voltage potentials are higher when the fillet size increases. Another approach to enhance the electric potential is by applying a higher voltage; however, this increases the risk of Joule heating [17]. Therefore, achieving improved performance at a relatively lower voltage, such as 5V, without escalating the voltage presents a significant advancement.

Table 2. Maximum and minimum voltages reached with respective to the fillet size

Fillet size [µm]	Maximum voltage [V]	Minimum voltage [V]
0	3.075	-0.935
3	3.087	-0.939
6	3.124	-0.958
9	3.184	-0.991
12	3.242	-1.048
15	3.253	-1.110
18	3.269	-1.178

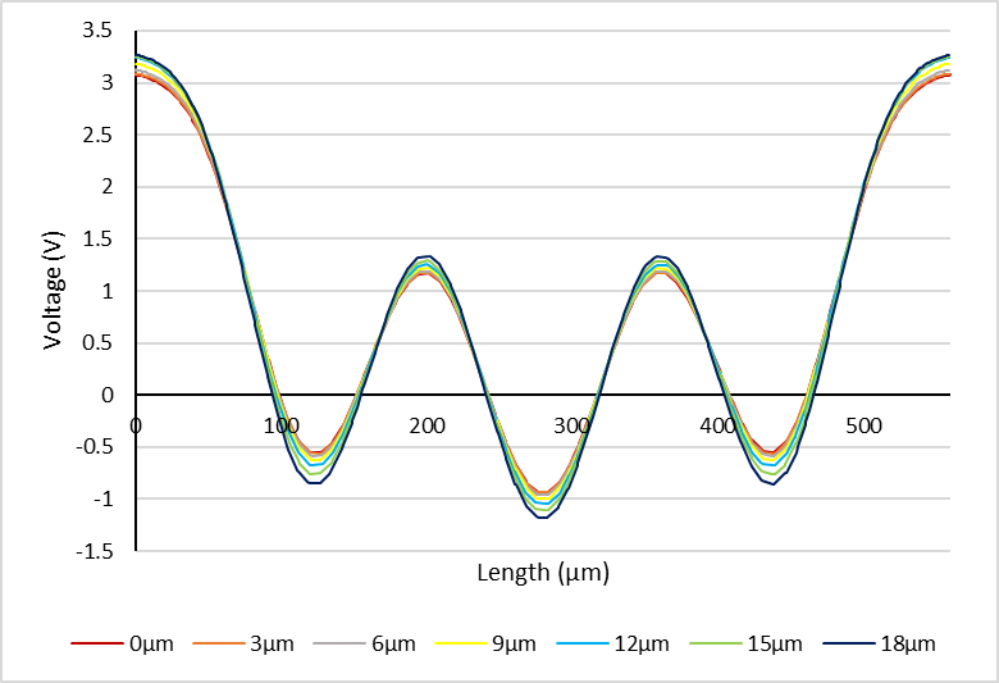

Figure 6. Electric potential vs arc length graphs for varying fillet radius

This trend suggests that optimizing electrode curvature can significantly impact the separation performance in the microchannel. Accelerating a cycle by few milliseconds can be crucial in medical applications, where real-time responses, precision, and throughput are essential. In POC devices and continuous monitoring systems, faster processing enhances diagnostic and therapeutic response times. Minor reductions in cycle times significantly boost throughput, making these improvements particularly valuable for high-volume biological sample processing and analysis. One of the challenges associated with DEP is the relatively low flow rate [14], which limits the throughput. This can be mitigated by accelerating

the separation process [27]. This study optimizes the electrode design, enabling faster separation, thereby improving the performance of DEP-based separation systems. The study employs NDEP, which minimizes particle damage compared to PDEP. In NDEP, particles are repelled from regions of high electric field strength, reducing their exposure to intense fields. PDEP can lead to particle adhesion [18] to the electrodes due to attraction to regions of high electric field strength, potentially causing damage to both the particles and the electrodes.

As this study is based on simulations, it is important to note that the results may not fully translate to experimental setups. Numerous studies have already demonstrated that experimental procedures rarely achieve 100% purity or efficiency [16, 20, 21]. Considering this study, several factors may affect the accuracy of simulations. Simulations operate under idealized conditions, whereas experimental setups can be influenced by variables such as temperature fluctuations, noise, or contamination. Maintaining boundary conditions such as perfect insulation can be challenging in practical scenarios. Additionally, in the simulations, particle flow at the inlet is defined by precise release timings, allowing particles to flow one at a time. In experimental setups, however, multiple particles may be released simultaneously, which could impact the separation results. Furthermore, the DEP force applied in the simulations is based on predefined particle properties and trajectories. In real-world experiments, slight variations in particle properties could influence DEP forces. Other forces that are neglected in the simulations might also act on the particles, further complicating the results.

Despite the widespread use of MEMS devices in various real-world applications such as accelerometers, gyroscopes, DNA sequencers, and pressure sensors, several challenges arise during the fabrication process. These challenges include issues related to cost, structural implementation failures, and chemical bonding between contact surfaces [28]. Fabrication constraints related to this study include fluid contamination, leakage, short circuit, and structural defects. This device's small size and precise features, particularly the electrodes, necessitate the use of high-end resources in the fabrication process. Furthermore, proper attention should be paid to the materials chosen for different device parts, including the electrodes. Material choice significantly impacts the reactions occurring at the electrodes and the dissipation of heat generated, such as Joule heating, which can cause complications such as expansions in the device structure [28, 29].

Conclusions

In this study, the separation of RBCs and platelets was achieved through theoretical analysis and COMSOL simulations, utilizing DEP and drag forces to guide particle trajectories toward designated outlets. The optimization of electrode geometry, specifically by introducing curvature and varying the fillet radius between 0 and 18 μm, significantly reduced the separation time while maintaining 100% separation efficiency for both RBCs and platelets across all simulations. This demonstrates the effectiveness of the proposed design in enhancing separation performance without sacrificing the separation efficiency. The introduction of curvature improved the separation performance by accelerating the separation process, which can be used to address a common DEP limitation: low throughput. This study emphasizes the critical role of electrode design in improving the performance of DEP-based systems, offering valuable insights for

future advancements in cell separation technologies. Future research can extend this work by applying the optimized design refining the model to achieve even higher throughput for practical applications. Additionally, future studies should investigate the underlying mechanisms for the accelerated separation observed, particularly the influence of the fillet radius on voltage distribution and the resulting impact on particle movement. By addressing these future directions, this research paves the way for developing more efficient and versatile DEP-based microfluidic separation systems.

Conflicts of Interest

The authors declare that there is no conflict of interest regarding the publication of this paper.

Acknowledgment

The authors would like to express their gratitude to the laboratory and research team at the University of Moratuwa for providing the necessary simulation tools and access to COMSOL Multiphysics 5.3a software.

References

[1] Zborowski, M. and Chalmers, J.J., Rare cell separation and analysis by magnetic sorting. Anal Chem, **2011**. 83*(21)*, 8050-6. 10.1021/ac200550d.

[2] Tomlinson, M.J., Tomlinson, S., Yang, X.B., and Kirkham, J., Cell separation: Terminology and practical considerations. J Tissue Eng, **2013**. 4, 2041731412472690. 10.1177/2041731412472690.

[3] Nurden, A.T., Nurden, P., Sanchez, M., Andia, I., and Anitua, E., Platelets and wound healing. Front Biosci, **2008**. 13, 3532-48. 10.2741/2947.

[4] Zucker, M.B., Pert, J.H., Lundberg, A., Yankee, R.A., and Henderson, E.S., Preservation and clinical use of platelets. Vox Sang, **1969**. 16*(4)*, 373-81. 10.1111/j.1423-0410.1969.tb04764.x.

[5] Byrnes, J.R. and Wolberg, A.S., Red blood cells in thrombosis. Blood, **2017**. 130*(16)*, 1795-1799. 10.1182/blood-2017-03-745349.

[6] Peter Klinken, S., Red blood cells. Int J Biochem Cell Biol, **2002**. 34*(12)*, 1513-8. 10.1016/s1357-2725(02)00087-0.

[7] Radisic, M., Iyer, R.K., and Murthy, S.K., Micro- and nanotechnology in cell separation. Int J Nanomedicine, **2006**. 1*(1)*, 3-14. 10.2147/nano.2006.1.1.3.

[8] da Silva, E.T.S.G., Souto, D.E.P., Barragan, J.T.C., de F. Giarola, J., de Moraes, A.C.M., and Kubota, L.T., Electrochemical Biosensors in Point-of-Care Devices: Recent Advances and Future Trends. ChemElectroChem, **2017**. 4*(4)*, 778-794. 10.1002/celc.201600758.

[9] Bogue, R., MEMS sensors: past, present and future. Sensor Review, **2007**. 27*(1)*, 7-13. 10.1108/02602280710722498.

[10] Luo, T., Fan, L., Zhu, R., and Sun, D., Microfluidic Single-Cell Manipulation and Analysis: Methods and Applications. Micromachines (Basel), **2019**. 10*(2)*, 104. 10.3390/mi10020104.

[11] Caglayan, Z., Demircan Yalcin, Y., and Kulah, H., A Prominent Cell Manipulation Technique in BioMEMS: Dielectrophoresis. Micromachines (Basel), **2020**. 11*(11)*, 990. 10.3390/mi11110990.

[12] Nguyen, N.V., Le Manh, T., Nguyen, T.S., Le, V.T., and Van Hieu, N., Applied electric field analysis and numerical investigations of the continuous cell separation in a dielectrophoresis-based microfluidic channel. Journal of Science: Advanced Materials and Devices, **2021**. 6*(1)*, 11-18. https://doi.org/10.1016/j.jsamd.2020.11.002.

[13] Lewpiriyawong, N. and Yang, C., AC-dielectrophoretic characterization and separation of submicron and micron particles using sidewall AgPDMS electrodes. Biomicrofluidics, **2012**. 6*(1)*, 12807-128079. 10.1063/1.3682049.

[14] Çetin, B., Kang, Y., Wu, Z., and Li, D., Continuous particle separation by size via AC-dielectrophoresis using a lab-on-a-chip device with 3-D electrodes. Electrophoresis, **2009**. 30*(5)*, 766-774.

[15] Zhang, Y. and Chen, X., Dielectrophoretic microfluidic device for separation of red blood cells and platelets: a model-based study. Journal of the Brazilian Society of Mechanical Sciences and Engineering, **2020**. 42*(2)*, 89. 10.1007/s40430-019-2114-4.

[16] Varmazyari, V., Habibiyan, H., Ghafoorifard, H., Ebrahimi, M., and Ghafouri-Fard, S., A dielectrophoresis-based microfluidic system having double-sided optimized 3D electrodes for label-free cancer cell separation with preserving cell viability. Scientific Reports, **2022**. 12*(1)*, 12100. 10.1038/s41598-022-16212-w.

[17] Shirmohammadli, V. and Manavizadeh, N., Application of Differential Electrodes in a Dielectrophoresis-Based Device for Cell Separation. IEEE Transactions on Electron Devices, **2019**. 66*(9)*, 4075-4080. 10.1109/TED.2019.2926829.

[18] Ling, S.H., Lam, Y.C., and Chian, K.S., Continuous Cell Separation Using Dielectrophoresis through Asymmetric and Periodic Microelectrode Array. Analytical Chemistry, **2012**. 84*(15)*, 6463-6470. 10.1021/ac300986q.

[19] Techaumnat, B., Panklang, N., Wisitsoraat, A., and Suzuki, Y., Study on the discrete dielectrophoresis for particle–cell separation. Electrophoresis, **2020**. 41*(10–11)*, 991-1001.

[20] Piacentini, N., Mernier, G., Tornay, R., and Renaud, P., Separation of platelets from other blood cells in continuous-flow by dielectrophoresis field-flow-fractionation. Biomicrofluidics, **2011**. 5*(3)*, 034122. https://doi.org/10.1063/1.3640045.

[21] Doh, I. and Cho, Y.H., A continuous cell separation chip using hydrodynamic dielectrophoresis (DEP) process. Sensors and Actuators A: Physical, **2005**. 121*(1)*, 59-65. https://doi.org/10.1016/j.sna.2005.01.030.

[22] Wang, Y., Zhao, K., Tong, N., and Wang, J., Separation of microalgae cells in a microfluidic chip based on AC Dielectrophoresis. Journal of Chemical Technology & Biotechnology, **2023**. 98*(1)*, 140-150.

[23] Iliescu, C., Yu, L., Tay, F.E.H., and Chen, B., Bidirectional field-flow particle separation method in a dielectrophoretic chip with 3D electrodes. Sensors and Actuators B: Chemical, **2008**. 129*(1)*, 491-496. https://doi.org/10.1016/j.snb.2007.11.023.

[24] Voldman, J., Electrical forces for microscale cell manipulation. Annu Rev Biomed Eng, **2006**. 8*(1)*, 425-54. 10.1146/annurev.bioeng.8.061505.095739.

[25] Das, D., Biswas, K., and Das, S., A microfluidic device for continuous manipulation of biological cells using dielectrophoresis. Medical Engineering & Physics, **2014**. 36*(6)*, 726-731. https://doi.org/10.1016/j.medengphy.2013.12.010.

[26] Islam, M., Natu, R., Larraga-Martinez, M.F., and Martinez-Duarte, R., Enrichment of diluted cell populations from large sample volumes using 3D carbon-electrode dielectrophoresis. Biomicrofluidics, **2016**. 10*(3)*, 033107. 10.1063/1.4954310.

[27] Kim, D., Kim, Y., Lee, D., Kim, B., and Lee, J., Electrode configuration optimization for maximizing throughput of dielectrophoretic particle separator. Journal of Mechanical Science and Technology, **2017**. 31*(12)*, 5951-5960. 10.1007/s12206-017-1133-3.

[28] Shoaib, M., Hamid, N.H., Malik, A.F., Zain Ali, N.B., and Tariq Jan, M., A review on key issues and challenges in devices level MEMS testing. Journal of Sensors, **2016**. 10.1155/2016/8142463.

[29] Ghomian, T. and Hihath, J., Review of Dielectrophoretic Manipulation of Micro and Nanomaterials: Fundamentals, Recent Developments, and Challenges. IEEE Trans Biomed Eng, **2023**. 70*(1)*, 27-41. 10.1109/TBME.2022.3183167.